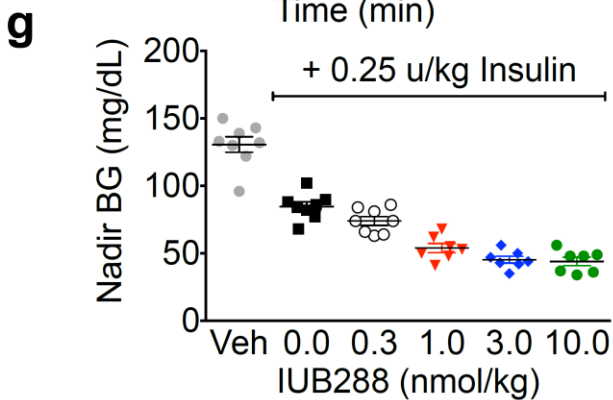
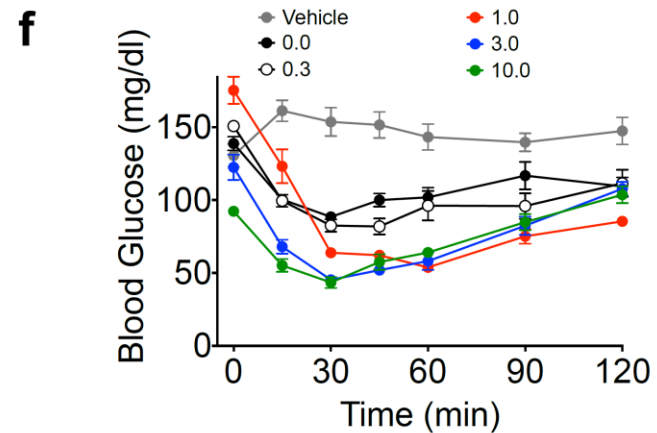
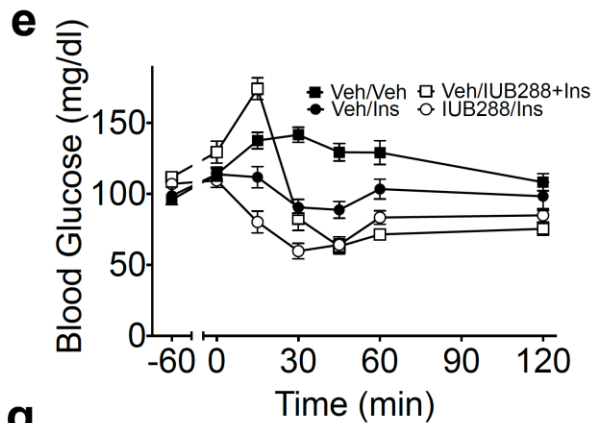
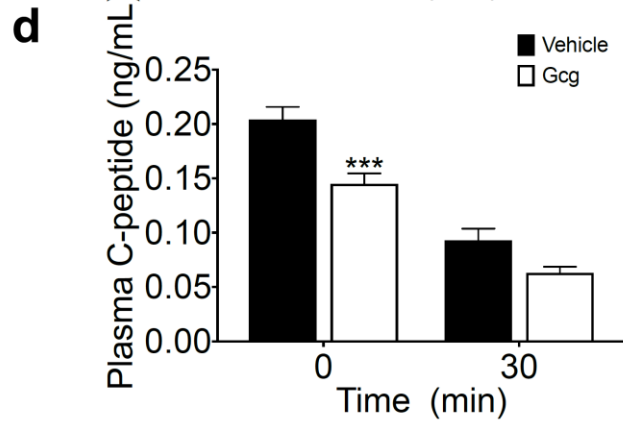
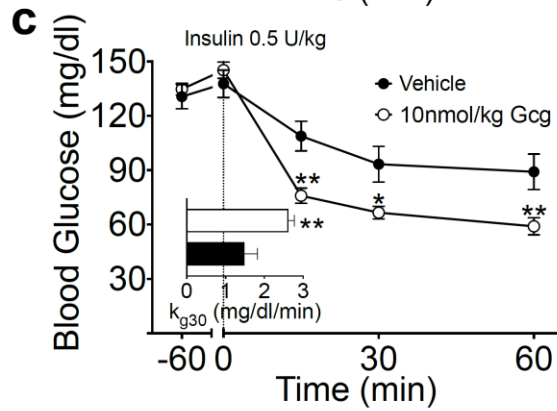
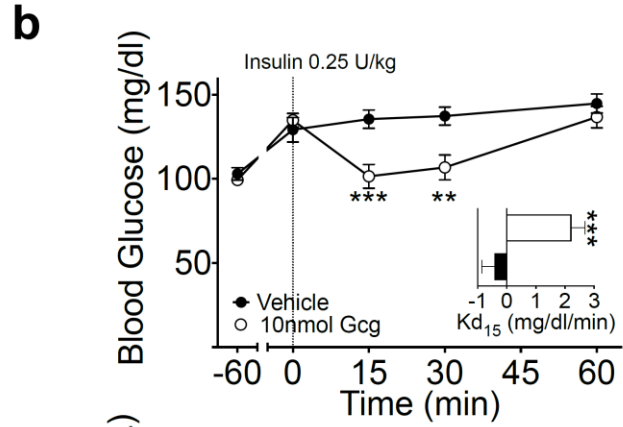
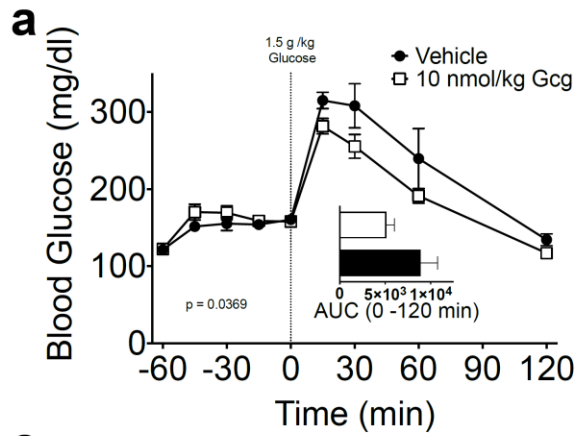


SUPPLEMENTARY DATA

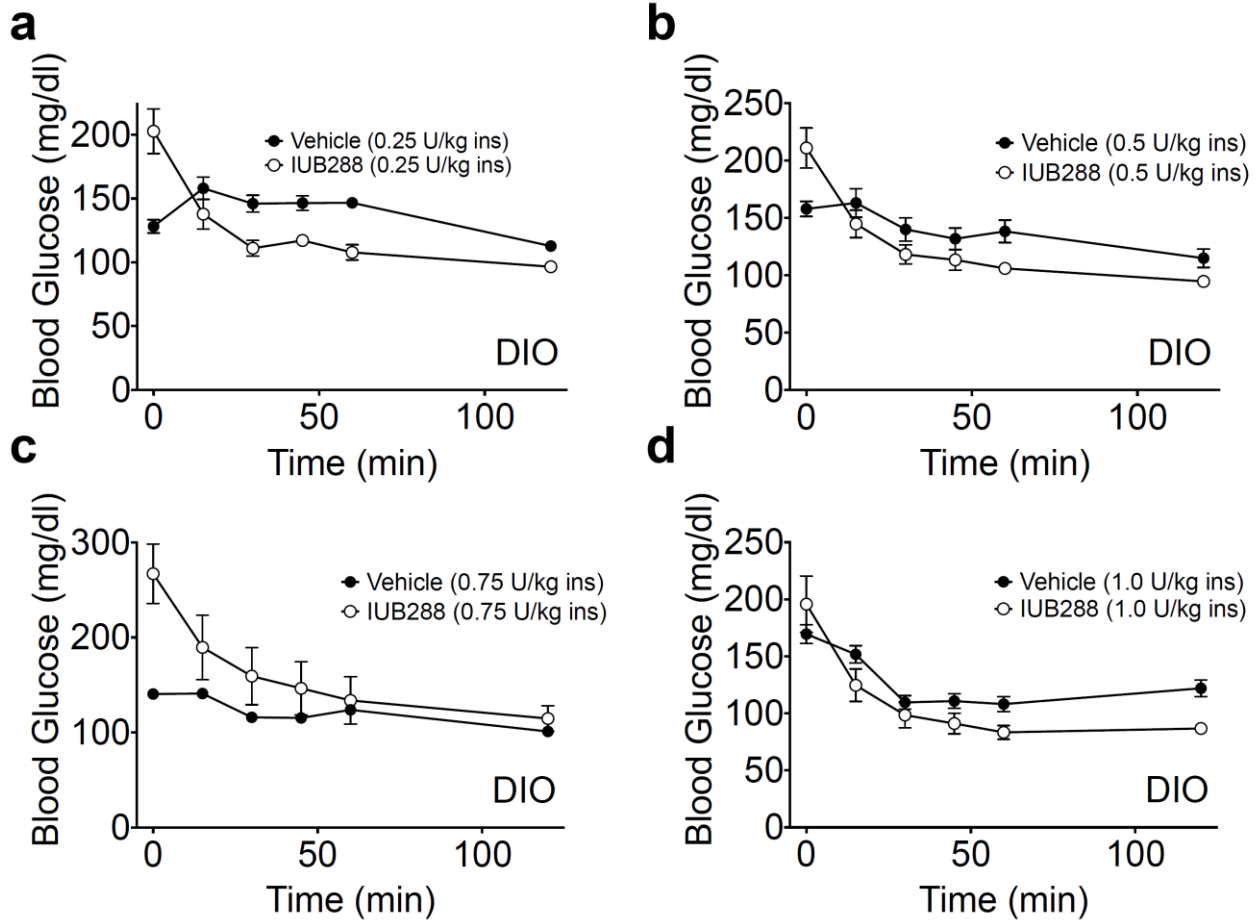
Supplementary Figure S1. The beneficial effects of acute GCGR agonism are Glucagon-specific. Glucose Tolerance Test (GTT) (a) and area under the curve analysis (a-inset) in C57Bl/6J mice with or without 60 min native glucagon (10nmol/kg) pretreatment (n=6). 0.25U/kg Insulin Tolerance Test (ITT) and kg15 (b), 0.5U/kg ITT and kg30 (c), and plasma C-peptide (d) during 0.5U/kg ITT in C57Bl/6J mice with or without 60 min glucagon (10nmol/kg) pretreatment (n=14-16). ip (0.25 U/kg) after IUB288 (10nmol/kg) and insulin co-treatment (e). ITT (0.25 U/kg) (f) and blood glucose nadir (g) in lean, chow-fed mice pretreated with various doses of IUB288 (0, 0.3, 1, 3, and 10nmol/kg) for 180 min (n=7-9). All data are represented as mean +/- SEM. * $p < 0.05$, ** $p < 0.01$, *** $p < 0.001$.

SUPPLEMENTARY DATA



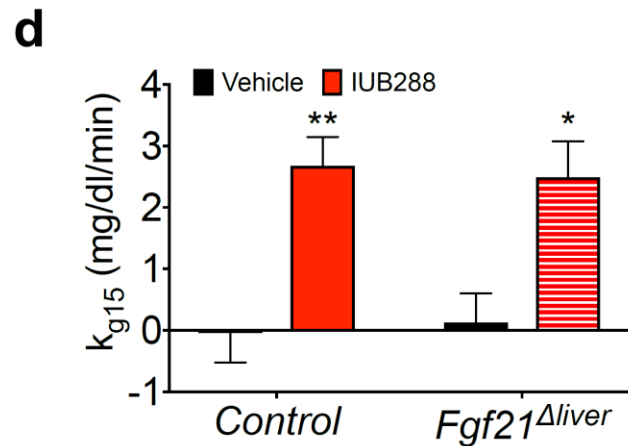
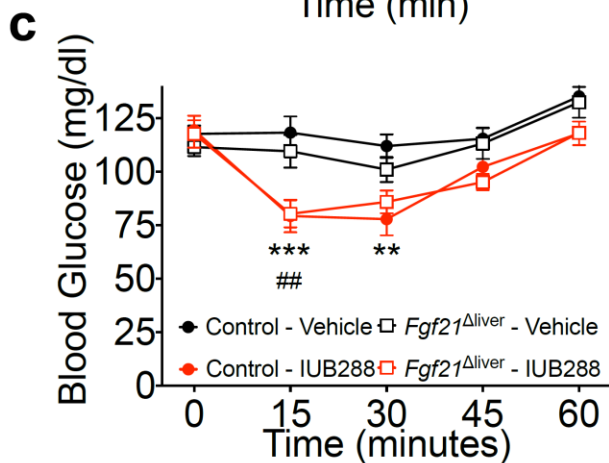
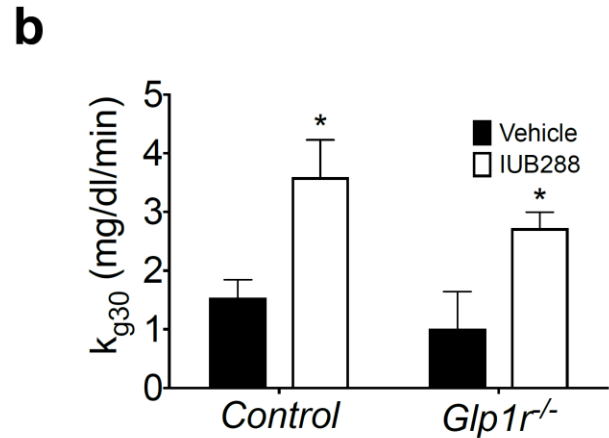
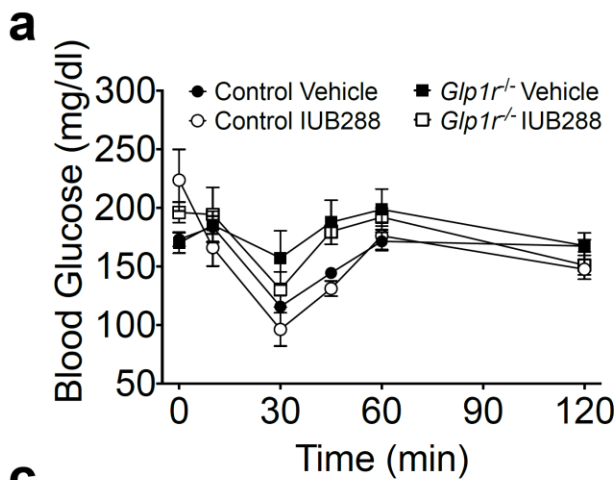
SUPPLEMENTARY DATA

Supplementary Figure S2. Acute GcgR agonism enhances insulin action in obese mice. Insulin Tolerance Test (ITT) at 0.25 (a), 0.50 (b), 0.75 (c), and 1.0 U/kg (d) insulin in DIO mice with single injection of IUB288 (10nmol/kg) at -60 min. All data are represented as mean \pm SEM. n=8 mice/group.



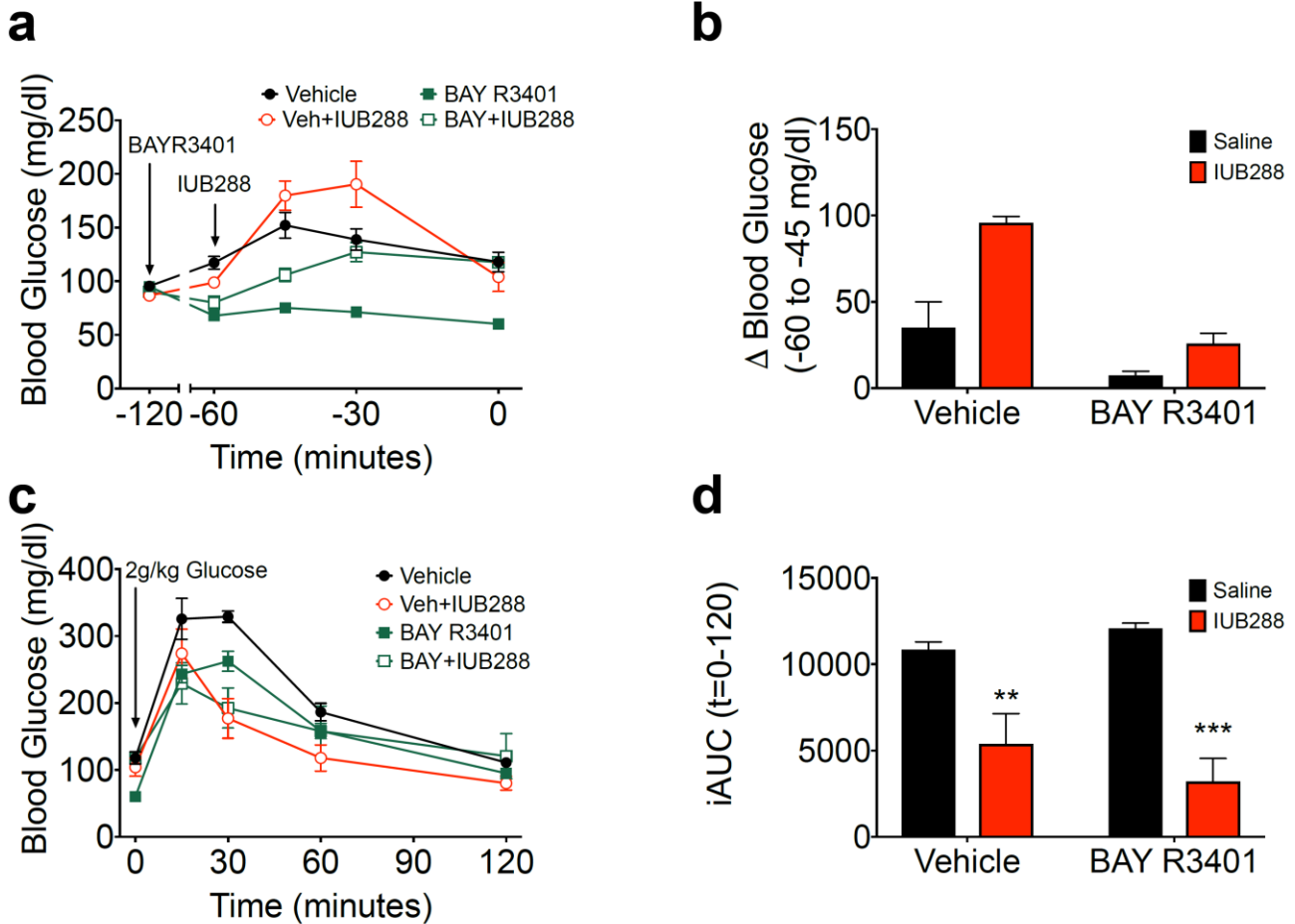
SUPPLEMENTARY DATA

Supplementary Figure S3. The beneficial effects of acute GcgR agonism are GLP1R and FGF21 independent. Insulin Tolerance Test (ITT) (0.25U/kg insulin) (a) and rate of glucose change (kg30, b) of Control and GLP1-R deficient mice with or without 60 min ip IUB288 (10nmol/kg) pretreatment. ITT (0.25U/kg insulin) (c) and rate of glucose change (kg15, d) of Control and *Fgf21*^{ΔLiver} mice with or without ip 60 min IUB288 (10nmol/kg) pretreatment. All data are represented as mean +/- SEM. *p< 0.05, **p< 0.01, ***p< 0.001 vs Control vehicle within time points, #p< 0.05 vs *Fgf21*^{ΔLiver} vehicle within time points.



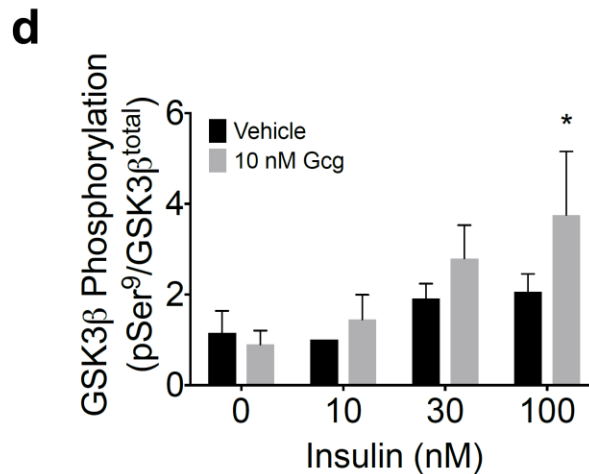
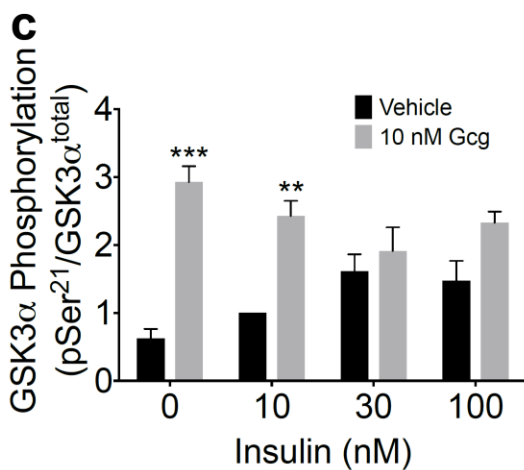
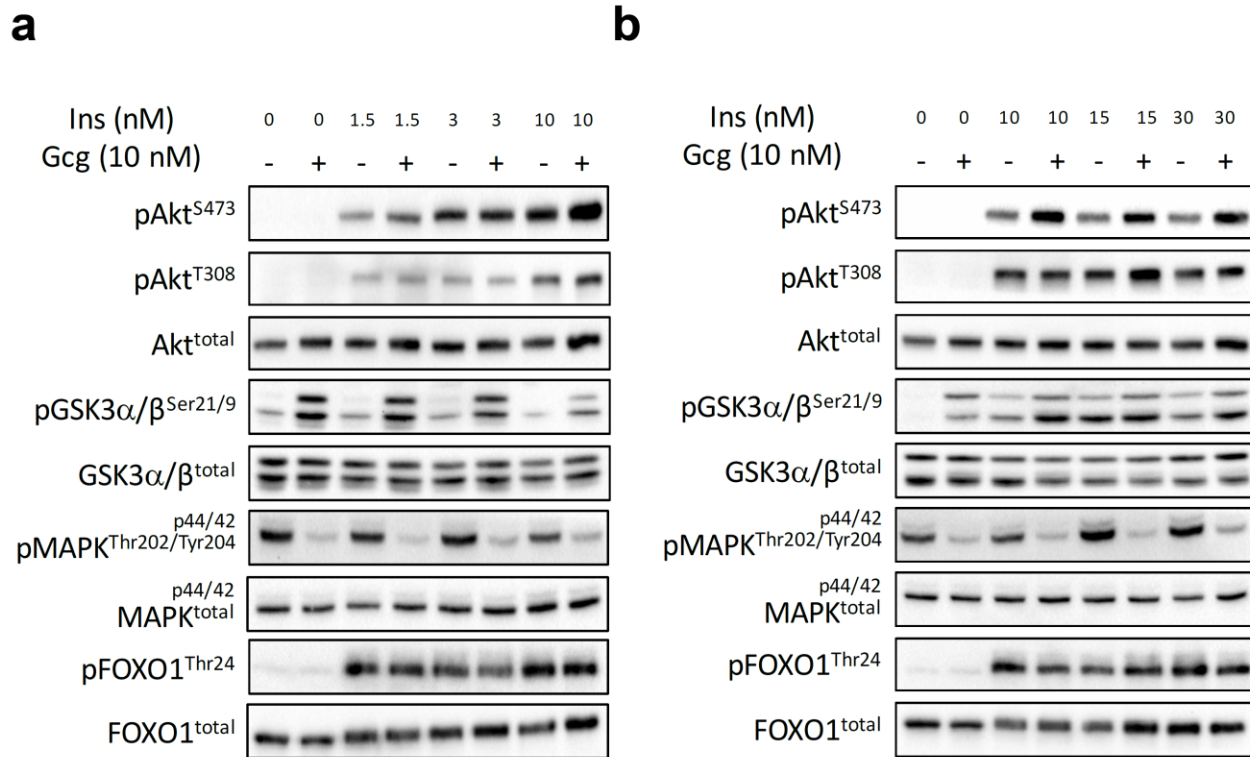
SUPPLEMENTARY DATA

Supplementary Figure S4. The beneficial effects of acute GcgR agonism are independent of glycogen depletion. Blood glucose excursion (a) and 15min change (b) in response to GcgR agonsim (10nmol/kg IUB288) in the presence or absence of glycogen phosphorylase a/b inhibitor (10mg/kg BAY R3401) in C57Bl/6J mice. GTT (2g/kg) (c) and area under the curve analysis (d) following ip glucose challenge IUB288- and BAY R3401-treated and control mice (n=6). All data are represented as mean +/- SEM, **p< 0.01, ***p< 0.001.



SUPPLEMENTARY DATA

Supplementary Figure S5. GcgR agonism enhances insulin action at GSK3. Immunoblot analysis of hepatocyte insulin signaling in response to low- (a) and high- (b) dose insulin and glucagon co-treatment. Representative images of 6 independent/observations. Immunoblot analysis of GSK3 α/β phosphorylation (c & d) in response to insulin and glucagon co-treatment in isolated hepatocytes (see Figure 3d). All data are represented as mean \pm SEM of 4 independent/observations. * $p < 0.05$, ** $p < 0.01$, *** $p < 0.001$.



Supplementary Figure S6. Insulin signaling during labeled, euglycemic clamp. Immunoblot analysis in liver, EDL, and BAT from clamped mice (Figures 3-4). Densitometric quantification (a-d) and representative images (e-g) of insulin signaling pathway components in 6-7 mice/group. * $p < 0.05$, ** $p < 0.01$.

